XVIII IMEKO WORLD CONGRESS
Metrology for a Sustainable Development
September, 17 – 22, 2006, Rio de Janeiro, Brazil

A MICHELSON INTERFEROMETER AS A CALIBRATION TOOL OF A RADIAL IN-PLANE DIGITAL SPECKLE INTERFEROMETER

Matías Roberto Viotti [1], *Armando Albertazzi G. Jr.* [1], *Ricardo Suterio* [2]

[1] Laboratório de Metrologia e Automação (LABMETRO), Universidade Federal de Santa Catarina (UFSC)
Cx. Postal 5053, CEP 88040-970, Florianópolis, SC, Brasil, mov@labmetro.ufsc.br.

[2] Laboratório de Integração e Testes (LIT), Instituto Nacional de Pesquisas Espaciais (INPE)
Cx. Postal 515, CEP 12227-010, São José dos Campos, SP, Brasil, suterio@lit.inpe.br.

Abstract: The paper reports on the use of a Michelson interferometer for calibration of a radial in-plane digital speckle pattern interferometer. Also presents a numerical method to calculate a correction factor from the assessment of the displacements measured with both interferometers. This factor allows correcting mistakes introduced in the measurement process and generated mainly by a laser diode, which is used as light source of the digital speckle pattern interferometer. The description of the experimental set up and calibration procedure are presented. Experimental results obtained during one calibration process are also given. Finally, it will be demonstrated that the calibrated RIP system can measure displacements with a smaller average deviation, once the experimental results were analyzed and the calibration process was carried out, since it diminished from 6.2 % up to 1.5 %.

Keywords: Michelson interferometer, ESPI, radial interferometer, length measurement.

1. INTRODUCTION

When physics and engineering students read several books about applied optics and light interference, they will find a great number of amplitude-shifting interferometers employed for different metrological and industrial uses. However, the Michelson interferometer is the best known and historically the most important among them [1]. It is widely utilized in laser technology for spectral analysis, laser frequency tuning and optical cavities [2, 3] as well for making accurate length measurements [4, 5].

In the last decades, several optical techniques have been developed that have the ability to generate fringe patterns from which the displacement field from can be evaluated. Among them, digital speckle pattern interferometry (DSPI) is the most versatile one [6]. As it is well known, DSPI is based on the generation of speckle distributions by a laser source. In contrast to holographic interferometry, which needs a photographic process, DSPI uses speckles sufficiently large to be resolved by a video system. The application of digital techniques in DSPI allows the automation of the data analysis process, which is usually based on the extraction of the optical phase distribution encoded by the generated correlation fringes [7]. From these data, in-plane and out-of-plane whole-field displacement fields can be measured over the surface of any rough object without making contact with it.

Albertazzi et al. [8-10] have developed a novel portable double illumination DSPI system (RIP interferometer), that allows to measure, with a single image, the complete radial in-plane displacement field in a point of interest. This field provides sufficient information for full characterization of the displacement, strain and stress fields in the interrogated region. As it was mentioned previously, the displacement field can be computed from the measured optical phase by using an expression that involves the magnitude of the wavelength of the laser used as light source [6]. This portable interferometer uses a cheap and small diode laser whose wavelength is not exactly known. In consequence, some mistakes can be introduced during the evaluation of the displacement fields.

This work presents a numerical calibration process, which has the objective to deal with these errors. As Michelson interferometer enables to determine lengths accurately, it was used as the tool to accomplish this calibration process. Thus, the displacement of a plate was monitored simultaneously with the radial in-plane interferometer and the Michelson one. Then, both measured displacements were computed, compared and analyzed in order to evaluate the measurement quality of the RIP interferometer and to obtain, whether it was necessary the correction factor that would allow avoiding measurement mistakes. This paper is organized as follows. First at all, both interferometers are described briefly as well as their working principles. Afterwards, the calibration procedure and its experimental results are presented. In the end, the analysis of the results and the main conclusions of them are shown.

2. RADIAL IN-PLANE INTERFEROMETER (RIP)

Figure 1 shows a cross section of the interferometer used to obtain radial in-plane sensitivity [8-10]. The most important component is a conical mirror, which is positioned near the specimen surface. This figure also displays two particular light rays chosen from the collimated

illumination source. Each light ray is reflected by the conical mirror surface towards a point P over the specimen surface, reaching it with the same incidence angle. The illumination directions are indicated by the unitary vectors $\mathbf{n_A}$ and $\mathbf{n_B}$ and the sensitivity direction is given by the vector **k** obtained from the subtraction of both unitary vectors. As the angle is the same for both light rays, in-plane sensitivity is reached at point P. Over the same cross section and for any other point over the specimen surface, it can be verified that there is only one couple of light rays that merge at that point. Also, in the cross section shown in Fig. 1, the incidence angle is always the same for every point over the specimen surface and symmetric with respect to the mirror axis. If the direction of the normal of the specimen surface and the axis of the conical mirror are parallel to each other, then $\mathbf{n_A}$ and $\mathbf{n_B}$ will have the same angle. Therefore, the sensitivity vector **k** will be parallel to the specimen surface and radial in-plane sensitivity will be obtained.

The above description can be extended to other cross sections of the conical mirror. If the central point is kept out from this analysis, it can be demonstrated that only one pair of light rays illuminate each point of the specimen surface. As both rays are coplanar with the mirror axis and symmetrically oriented to it, therefore full 360º radial sensitivity is obtained for a circular region over the specimen.

A practical configuration of the radial in-plane interferometer is shown in Fig. 2. The light from a 50 mW diode laser with a wavelength of 658 nm is expanded and collimated via two convergent lenses and the collimated beam is reflected towards the conical mirror by a mirror that forms a 45º angle with the axis of the conical mirror. The central hole placed at this mirror prevents that the laser light reaches directly the sample surface having triple illumination and provides a viewing window for the CCD camera.

The intensity of the light is not constant over the whole circular illuminated area on the specimen surface and it is particularly higher at the central point because it receives light contribution from all cross sections. As a result, a very bright spot will be visible at the central part of the circular measurement region and consequently fringe quality will be reduced. To reduce this effect, two parts form the conical mirror with a small gap between them. The distance of this gap is adopted in such a way that the light rays reflected to the center are blocked. Thus, a small circular shadow is created in the center of the illuminated area and fringe blurring is avoided.

As it can be seen from Fig. 2, for each point over the specimen the two rays of the double illumination are originated from the reflection of the upper and lower parts of the conical mirror. A piezoelectric actuator (PZT) was used to join the upper part of the conical mirror, so that its lower part is fixed while the upper part is mobile. As a consequence, the PZT moves the upper part of the conical mirror along its axial direction and the gap between both parts is increased. Then, a small optical path change between both light rays that intersect on each point is produced and the PZT device allows the introduction of a phase shift to evaluate the optical phase distribution by means of the Carré algorithm [7]. As it is well known, this phase-shifting method assumes that the phase shifts introduced between successive speckle interferograms are all equal. Thus, four speckle interferograms are sufficient to evaluate the optical phase distribution.

The angle between the directions of illumination and the normal to the specimen surface is chosen as 60º. The test specimen surface is monitored lively by a CCD camera, whose output is digitized by a frame grabber with a resolution of pixels and 256 gray levels (8bits). This camera provides a field of view that includes the illuminated area of 10 mm in diameter over the specimen.

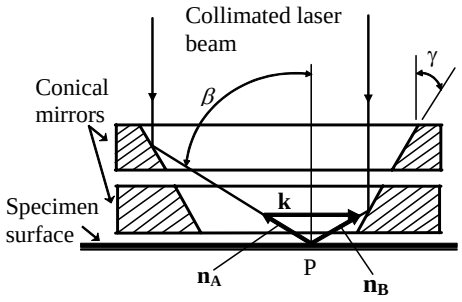

Fig. 1 - Cross section of the upper and lower parts of the conical mirror to show the radial in plane sensitivity of the interferometer.

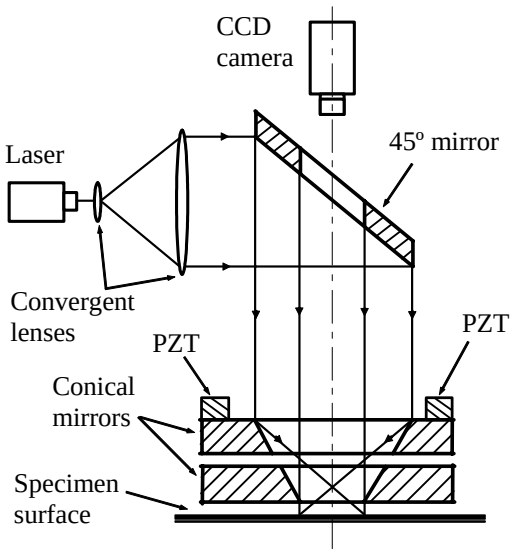

Fig. 2 - Optical setup of the radial in-plane interferometer.

3. MICHELSON INTERFEROMETER

The Michelson interferometer is a device that allows length measurement with high accuracy. Its configuration is shown schematically in Fig. 3.

The output of a He-Ne laser (*La*), with a wavelength of $\lambda = 632.8$ nm and a power of 35 mW, is divided into two symmetric beams by a beam splitter (*BS*). Then, the beam of the mobile arm travels the distance d_1 up to the mobile mirror M_1, where it is reflected, returning to the beam splitter. In the other hand, the beam of the fix arm goes to the fix mirror M_2 travelling the distance d_2 and being reflected to the beam splitter, too. Part of the beam coming

from M_1 passes through the beam splitter going downward and part of the wave coming from M_2 is deflected by *BS* toward the CCD camera. Thus, the two beams are united and interference can be expected due to the optical path difference between both arms, which is $d = 2(d_1 - d_2)$. The fringes are projected on a plate *Pl*, which is imaged by a CCD camera whose output is digitised by a Matrox Pulsar frame grabber located inside a personal computer, with a resolution of 512 x 512 pixels and 256 grey levels (8 bits). The linear displacements of the mirror M_1, which are controlled by means of a control unit, are produced by means of the piezoelectric transducer (*PZT*). As it is well known, an interference pattern typically consists of quite a large number of alternatively bright and dark fringes. A particular fringe corresponds to a fixed order *m*.

As M_1 is moved toward *BS*, the distance d_1 decreases. In consequence, the fringe with the highest order disappears whether *d* decreases by $\lambda/2$.

Each remaining fringe broadens as more and more fringes vanish. By the time $d = 0$ has been reached, the central fringe will have spread out filling the whole field of view of the CCD camera. Moving M_1 still farther causes the fringes reappear and move outward. Thus, every displacement introduced on the mobile mirror moves the fringes imagined by the camera. It is possible to know exactly the displacement applied to the mobile mirror M_1 by counting the number of fringes (*NF*) that has passed over the plate *Pl* and by using the following equation [1]

$$d = \frac{1}{2}\lambda.NF \qquad (1)$$

However, the Michelson interferometer would be used as a pattern tool to measure displacements and calibrate the DSPI system presented in the previous section, if the measurement uncertainties of the former were not larger than 10 % of the ones for the latter [11]. For this reason, a small modification is introduced in the interferometer of Fig. 3. The set up of the resulting configuration is shown in Fig. 4. Hereafter, the interferometer of Fig. 3 will be called as Simple Michelson Interferometer, and the one of Fig. 4 as Modified Michelson Interferometer.

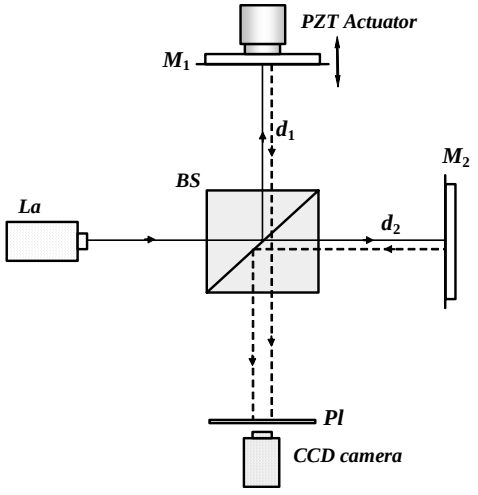

Fig. 3 - Scheme of the Michelson interferometer.

To obtain the modified Michelson interferometer, the mobile mirror M_1 is turned around its vertical axis and a fixed mirror M_3 is positioned in front of M_1 producing several reflections of the beam. This fact allows increasing the sensitivity of the interferometer and generating a larger number of fringes for the same displacement. By comparing the sensitivity of both interferometers, it can be seen that it is raised to about 7.8 times. In consequence, if one fringe is counted for a displacement of the mobile mirror M_1 for the simple Michelson interferometer, approximately 7.8 fringes will be counted for the modified one applying the same displacement over M_1.

It is important to highlight that Figs. 3 and 4 are only schemes of the interferometers, therefore the rays indicated with solid and dot lines go and come back along the same paths. The difference between them it is introduced to clarify these schemes.

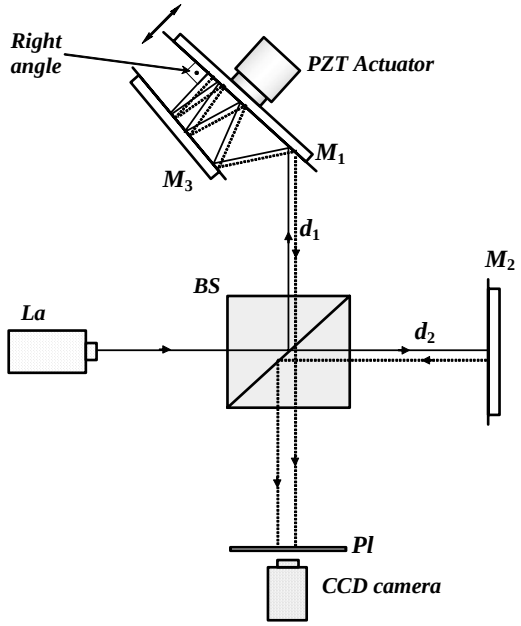

Fig. 4 - Set up of the modified Michelson interferometer.

4. EXPERIMENTAL PROCEDURE AND RESULTS

As it was explained in the previous section, the modified Michelson interferometer is used instead of the simple one to make the calibration due to the increase of its the sensitivity and its capacity to generate a larger number of fringes for the same displacement. However, to be applied as a calibration tool, this modified interferometer must be calibrated previously with the simple Michelson interferometer. In order to accomplish these process 15 different displacements were applied over the mirror M_1 and their respective number of fringes was measured with both Michelson interferometers producing 15 couples of measured displacements. According to Eq. 1, the displacement was evaluated from the number of fringes for the simple Michelson interferometer as follows

$$d = \frac{1}{2}\lambda_{He-Ne}.NF \qquad (2)$$

where the wavelength is the one of the He-Ne laser. The increase of sensitivity between both Michelson interferometers can be expressed as

$$IS = \frac{NF_{MM}}{NF} \tag{3}$$

NF and NF_{MM} are respectively the number of fringes measured by the simple and modified Michelson interferometers. Thus, Eq. 2 takes the form

$$d = \frac{1}{2}\lambda_{He-Ne} \cdot \frac{NF_{MM}}{IS} = \frac{1}{2}\lambda_{MM} .NF_{MM} \tag{4}$$

being λ_{MM} the wavelength that permits to compute the magnitude of the translation from the fringes measured with the modified Michelson interferometer. In consequence, the use of the increase of sensitivity enables to refer the simple interferometer to quantify the displacements with the modified one.

Figure 5 shows schematically how the Michelson interferometer and the radial in-plane digital speckle pattern one were positioned in order to accomplish the measurements. It can be seen that the mobile mirror M_1 of the simple and combined Michelson interferometers is joined to the piezoelectric actuator and to a horizontal plate *S*. This plate is moved in both directions (indicated for the arrow) with the combined system formed by the *PZT* actuator and the spring *Spg*. The radial in-plane interferometer is placed over the plate *S* to measure the in-plane translations introduced with the system *PZT-Spg*.

To perform the measurements, the following experimental procedure was used. First of all, the test plate *S* was positioned with the *PZT* in a reference point and the in-plane interferometer was fixed over this plate. Afterwards, a set of 4 phase-shifted speckle interferograms was acquired and the reference phase distribution was calculated by means of the Carré algorithm [7] and stored in a computer. Next, the mirror M_1 was displaced a determined distance by the *PZT* producing the movement of the fringes generated with the simple and modified Michelson interferometers (according to the explanation of the previous section). By the time, the displacement was taking place fringes were counted using the *CCD* camera and a computer acquisition program. After this, a second set of 4 phase-shifted speckle interferograms was acquired with the DSPI system and a new phase distribution was calculated and stored. Afterwards, the wrapped and continuous phase difference map was evaluated. Finally, the radial in-plane displacement field was evaluated from the continuous phase distribution by using [6]

$$u_r(r,\theta) = \frac{\phi(r,\theta)\,\lambda}{4\pi \sin\beta} \tag{5}$$

where $u_r(r,\theta)$ is the radial in-plane displacement field, $\phi(r,\theta)$ is the phase distribution, λ is the wavelength of the diode laser, β is the angle between the illumination directions and the normal of the specimen surface, and r and θ are the polar coordinates.

As an example, Fig. 6 shows the wrapped phase map obtained for displacement of 1.378 μm. The white arrow indicates the direction of the translation.

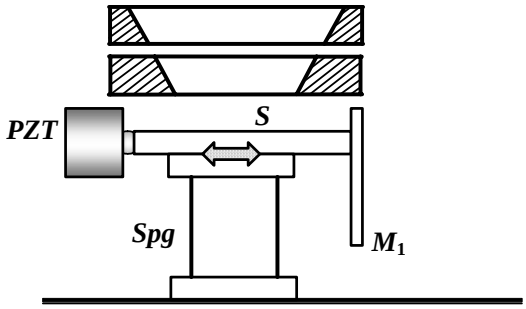

Fig. 5 - Experimental set up including the system to introduce translations and the position of the conical mirrors of the radial in-plane interferometer.

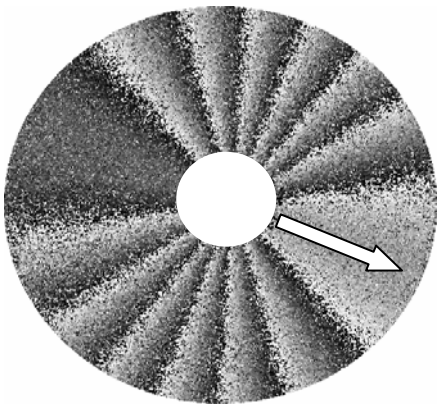

Fig. 6 - Wrapped phase distribution obtained for a translation (white arrow) of 1.378 μm.

Since the modified Michelson interferometer and the radial in-plane digital speckle interferometer monitored simultaneously the translation of the plate *S*, both measured displacements have to be the same. Thus, if these displacements are plotted in a 2D-graph, the resultant curve will be a line with a slope of 1. To understand this affirmation it is important to highlight that the displacements measured by the modified interferometer and by the digital speckle interferometer are placed in *y*- and *x*-axis of the graph, respectively. When both displacements are different, the slope will be different of 1. Fig. 7 shows the plot of a set of 52 displacements measured with both interferometers as well as the curve resulting of linear fitting. It can be seen that this curve has a slope of 0.9527. In order to correct these mistakes, a correction coefficient with a value of 1.04964 was introduced during the evaluation of the displacement field from of the optical phase distribution measured with the radial in-plane digital speckle pattern interferometer [Eq. (5)].

Once the calibration procedure was carried out, the optical phase distributions obtained for each translation of the plate *S* (Fig. 6), were processed and the magnitude of the displacements was quantified.

Figure 7 shows the comparison results. The corrected magnitude of displacement measured with RIP and the magnitude of the same displacement measured with the combined Michelson interferometer it can be noted that the radial in-plane interferometer can compute displacements with an average deviation of approximately 1.5 %. Previously to the calibration, the average deviation was

about 6.3 %. Fig. 8 shows the plot of the new deviation obtained for each measured translation.

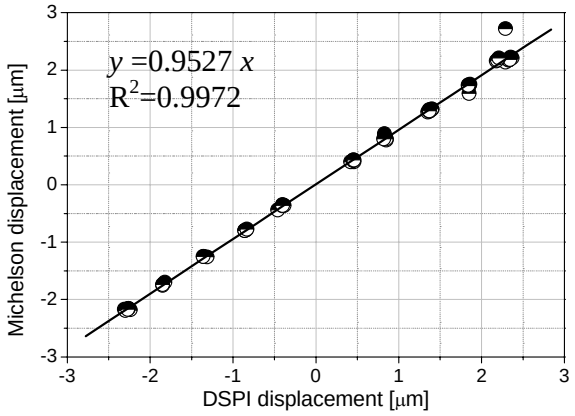

Fig. 7 - Plot of the measured displacements. (◓) experimental data, and (▬) linear fitting.

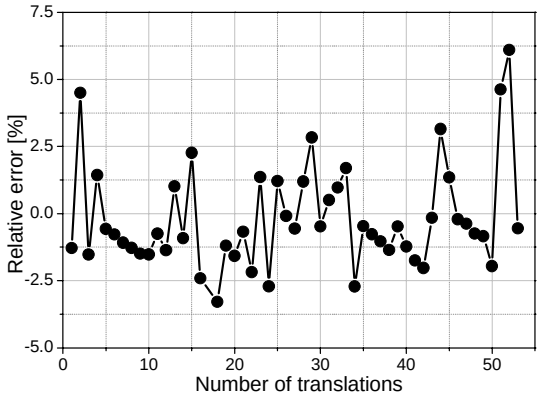

Fig. 8 - Plot of the average deviation for each measured translation.

5. CONCLUSION

The RIP system calibrated presented in this work is a valuable tool to measure the complete radial in-plane displacement field in a point where it is necessary to know and characterize the strain and stress fields presented into it. In the previous sections, it was indicated that the displacements field can be computed from the measured optical phase by using an expression that involves the magnitude of the wavelength of the laser used as light source. As the light source of this portable interferometer is a diode laser some mistakes can be introduced during the evaluation of the displacements fields.

In order to evaluate these possible mistakes, translations of a plate were measured with the RIP system and a modified Michelson interferometer. Thus, it was possible to see that the measurements had an average deviation of about 6.3 %. In consequence, a calibration process that is presented in this paper was applied to decrease this error to 1.5 %. According to the obtained results, it can be noted that the proposed calibration system has allowed improving the evaluation of the displacements fields measured with the radial in-plane interferometer since the average deviation diminished considerably respect to the previous one.

ACKNOWLEDGEMENTS

This research work was supported by a grant from the Conselho Nacional de Desenvolvimento Científico e Tecnológico (CNPq) of Brazil. The authors are also grateful to the technicians of the LABMETRO for their important help during the development of the research.

REFERENCES

[1] K. Aït-Ameur and F. Sanchez. “Transverse effects as source of error in coherence length measurements”. Opt Communic 233: pp 39-43, 2004.

[2] E.O. Doebelin, “Measurement systems: Application and Design”. Forth edition. Mc Graw-Hill; 1990.

[3] E. Hecht and A. Zajac. “Optics”. Addison-Wesley; 1974.

[4] O.G. Helles, P. Benech and R. Rimet. “Interferometric displacement sensor made by integrated optics and glass”. Sensors and actuators A: Physical; 47: pp 478-481, 1995.

[5] J.M. Huntley. “Automated analysis of speckle interferograms”. In: P.K. Rastogi, editor. Digital Speckle Pattern Interferometry and Related Techniques. Chichester: Wiley, New York; pp 59-139, 2001.

[6] P.K. Rastogi. “Measurement of static surface displacements, derivatives of displacements and three-dimensional surface shapes. Examples of applications to non-destructive testing”. In P.K. Rastogi, editor, Digital Speckle Pattern Interferometry and Related Techniques. Chichester:Wiley, New York; 2001.

[7] P.J. Rodrigo, M. Lim, and C. Saloma. “Optical-feedback semiconductor laser Michelson interferometer for displacements measurements with directional discrimination”. Appl Opt; 40: pp 506-513, 2001.

[8] A. Albertazzi G. Jr., M.R. Borges and C. Kanda, “A radial in-plane interferometer for residual stresses measurement using ESPI”. In Proc of SEM IX Int. Congress on Exp. Mech., Society of Experimental Mechanics; pp108-111, 2000.

[9] R. Suterio, A. Albertazzi G. Jr., F.K. Amaral and A. Pacheco. “Residual stress measurement using indentation and a radial in-plane ESPI interferometer”. In Proc of SPIE 8th International Symposium on Laser Metrology, Macro, Micro and Nano-Technologie Applied in Science; vol 5776: pp14-18, 2005.

[10] M.R. Viotti, A. Albertazzi G. Jr. and G.H. Kaufmann, “Measurement of residual stresses using local heating and a radial in-plane speckle interferometer”. Opt Eng 44 (9) 2005

[11] L. Zeng, K. Seta, H. Matsumoto and S. Iwashaki. “Length measurement by two-colour interferometer using two close wavelengths to reduce errors caused by air turbulence”. Meas Sci Technol;10: pp 587-591, 1999.